

Revealing Different Bonding Modes of Self-Assembled Octadecylphosphonic Acid Monolayers on Oxides by Time-of-Flight Secondary Ion Mass Spectrometry: Silicon vs Aluminum

Heng-Yong Nie*

Surface Science Western, Room G-1, WSC, The University of Western Ontario, London, Ontario N6A 5B7, Canada, and Department of Physics and Astronomy, The University of Western Ontario, London, Ontario N6A 3K7, Canada

Condensed octadecylphosphonic acid (OPA) dimers, i.e., two OPA molecules combined with the loss of a water molecule, were detected by time-of-flight secondary ion mass spectrometry (TOF-SIMS) on OPA self-assembled monolayers (SAMs) that are only weakly bonded on the native oxide layer of a silicon wafer. In contrast, these condensed dimers were absent on OPA SAMs formed on the oxide layer of an aluminum film, where the OPA molecules are chemically bonded on the substrate through a P–O–Al linkage. These observations lead us to conclude that the OPA molecules in their SAMs have to be free from chemical bonding with the substrate in order for the primary ion beam to generate ion fragments of the condensed dimer. We demonstrate that the detection of condensed OPA dimers serves as an analytical criterion for TOF-SIMS to reveal the bonding mode of OPA molecules in their SAMs on different oxides.

Self-assembled monolayers (SAMs) of organic molecules formed on a solid surface are an important model system in understanding self-assembly of molecules in terms of the interaction between the functional group of the molecules and the substrate.^{1,2} On the other hand, applications of SAMs have spread in a wide variety of areas, such as analytical chemistry, tribology, biology, nanotechnology, and organic electronics.^{3–10} Because of the importance of SAMs as a functioning molecular monolayer, continuing to develop analytical techniques to understand their formation mechanism on different substrates will help us to further

expand their applications. When molecules are delivered by a solution, the solvent may or may not impact the self-assembly of the molecules on a specific substrate, depending on the interactive strength between the functional group of the molecule and the substrate.¹¹ This is evident in the conventional methods for SAM formation, which require strong molecule–substrate interactions (by selecting molecule–substrate combinations): alkanethiols on noble metals (especially Au) and alkylsilanes on oxides (especially SiO₂).^{1,2,12,13} The linkage of the molecule to the substrate, S–Au for alkanethiols on gold, and Si–O–Si for alkylsilanes on SiO₂, are covalent bonds in nature. It has been shown that intermolecular interactions and molecule–substrate interactions impact the quality and stability of alkanethiol SAMs on Au.¹⁴ The key in SAM formation is thus to exploit specific interaction between the substrate and the headgroup of molecules of interest in a solution, in which the molecules are well dissolved and the substrate is immersed. Making weakly bonded SAMs on a substrate is thus out of the question in the context of the conventional SAM formation approaches. Obviously, other mechanisms have to be adopted to enable the formation of an ordered molecular monolayer that can only be weakly bonded to a substrate. To some extent, for example, the Langmuir–Blodgett approach allows perhaps more versatile molecule–substrate combinations because it transfers a molecular monolayer already formed (squeezed) on a subphase (e.g., water) to a substrate.^{13,15}

Organophosphorus acids have attracted much attention as they can form SAMs on various metal (M) oxides through P–O–M linkages.^{16–23} Among organophosphorus acids, *n*-octadecylphos-

* Corresponding author. E-mail: hnie@uwo.ca.

- Ulman, A. *Chem. Rev.* **1996**, *96*, 1533–1554.
- Schreiber, F. *Prog. Surf. Sci.* **2000**, *65*, 151–256.
- Gooding, J. J.; Mearns, F.; Yang, W. R.; Liu, J. Q. *Electroanalysis* **2003**, *15*, 81–96.
- Ashurst, W. R.; Yau, C.; Carraro, C.; Lee, C.; Kluth, G. J.; Howe, R. T.; Maboudian, R. *Sens. Actuators, A: Phys.* **2001**, *91*, 239–248.
- Whitesides, G. M.; Ostuni, E.; Takayama, S.; Jiang, X. Y.; Ingber, D. E. *Annu. Rev. Biomed. Eng.* **2001**, *3*, 335–373.
- Kelley, T. W.; Boardman, L. D.; Dunbar, T. D.; Muires, D. V.; Pellerite, M. J.; Smith, T. Y. P. *J. Phys. Chem. B* **2003**, *107*, 5877–5881.
- Liu, G. Y.; Xu, S.; Qian, Y. L. *Acc. Chem. Res.* **2000**, *33*, 457–466.
- Ma, H.; Acton, O.; Ting, G.; Ka, J. W.; Yip, H.-L.; Tucker, N.; Schofield, R.; Jen, A. K.-Y. *Appl. Phys. Lett.* **2008**, *92*, 113303.
- Klauk, H.; Zschieschang, U.; Pflaum, J.; Halik, M. *Nature* **2007**, *445*, 745–748.
- Goetting, L. B.; Deng, T.; Whitesides, G. M. *Langmuir* **1999**, *15*, 1182–1191.

- Nie, H.-Y.; Walzak, M. J.; McIntyre, N. S. *J. Phys. Chem. B* **2006**, *110*, 21101–21108.
- Nuzzo, R. G.; Allara, D. L. *J. Am. Chem. Soc.* **1983**, *105*, 4481–4483.
- Maoz, R.; Sagiv, J. *J. Colloid Interface Sci.* **1984**, *100*, 465–496.
- Barrena, E.; Palacios-Lidon, E.; Munuera, C.; Torrelles, X.; Ferrer, S.; Jonas, U.; Salmeron, M.; Ocal, C. *J. Am. Chem. Soc.* **2004**, *126*, 385–395.
- Zasadzinski, J. A.; Viswanathan, R.; Madsen, L.; Garnæs, J.; Schwartz, D. K. *Science* **1994**, *263*, 1726–1733.
- Mutin, P. H.; Guerrero, G.; Vioux, A. *J. Mater. Chem.* **2005**, *15*, 3761–3768.
- Thissen, P.; Valtiner, M.; Grundmeier, G. *Langmuir* **2010**, *26*, 156–164.
- Textor, M.; Laurence Ruiz, L.; Rossi, A.; Feldman, K.; Hahner, G.; Spencer, N. D. *Langmuir* **2000**, *16*, 3257–3271.
- Murase, A.; Ohmori, T. *Surf. Interface Anal.* **2001**, *31*, 93–98.
- Viomery, C.; Chevolut, Y.; Leonard, D.; Aronsson, B.-O.; Pechy, P.; Mathieu, H. J.; Descouts, P.; Gratzel, M. *Langmuir* **2002**, *18*, 2582–2589.
- Adden, N.; Gamble, L. J.; Castner, D. G.; Hoffmann, A.; Gross, G.; Menzel, H. *Langmuir* **2006**, *22*, 8197–8204.

phonic acid (OPA or ODPA) has been a model molecule for studies of formation mechanisms of SAM on oxides. For example, formation of OPA SAMs on a freshly cleaved mica surface using polar solvents as the delivering medium has been well studied; however, it has proven that no full-coverage OPA SAMs can be achieved.^{24–26} In contrast, with nonpolar solvents having a dielectric constant around 4, it has been demonstrated that even a weakly bonded self-assembly of OPA monolayer, with full coverage, can be achieved on the native oxide layer of a Si wafer, for which the conventional methods yield liquid-like stacks of OPA molecules because of the lack of strong interaction between the molecular headgroup and the silicon oxide.^{11,27–30} It is worth noting that this SAM formation approach facilitates an extremely fast process so that spin-coating and dip-coating approaches can be adopted. The concentration and alignment of the polar OPA headgroup on the nonpolar medium surface are believed to be the driving force for the fast growth of SAMs on a hydrophilic substrate.¹¹ Because of this situation realized by the “right” dielectric constant of the solvent,³¹ the delivering medium only allows the interaction between molecular headgroup and the hydrophilic surface of the substrate.¹¹

It has been demonstrated that the nature of the attachment (or bonding mode) of the OPA headgroup to different oxides varies, for example, from chemical bonding of P–O–Al linkage through a condensation reaction^{16,32,33} for OPA SAMs on an oxidized Al surface to hydrogen bonding (H-bonding) for OPA SAMs on an oxidized Si surface.¹¹ Regardless of the diversity in the bonding mode of OPA molecules on different oxides, the OPA SAMs themselves are closely packed and have a crystalline-like structure terminated by well-ordered methyl groups.

Because of its ability to probe a molecular monolayer on a substrate, time-of-flight secondary ion mass spectrometry (TOF-SIMS)³⁴ has been successfully applied to studies of SAM systems, such as thiols^{35–40} on Au, organosilanes⁴¹ on oxidized Al, as well as organophosphorus acids^{18–23} on various oxides of metals, such as Al, Fe, Ti, Ta, and Hf. Ion fragmentation of SAMs generated by the primary ion beam bombardment verifies the presence of molecules and provides clues to elucidate the interaction between the molecular headgroup and the substrate. In all these studies, the molecules are covalently bonded on the substrate. By taking advantage of our ability to prepare OPA SAMs either weakly

bonded on oxidized Si or covalently bonded on oxidized Al, we report for the first time that TOF-SIMS can be used to reveal these different bonding modes (i.e., speciation of molecules) of OPA molecules on these different oxides. Particularly, we prove that the condensed OPA dimer (i.e., two OPA molecules combined with the loss of one water molecule), detected as both positive and negative secondary ion fragments, serves as the signature for weakly bonded OPA SAMs on oxidized Si. This species is absent for OPA SAMs on oxidized Al, where strong chemical bonding dominates.

EXPERIMENTAL SECTION

Used in this study was *n*-octadecylphosphonic acid [$\text{CH}_3(\text{CH}_2)_{17}\text{P}(\text{O})(\text{OH})_2$, purity >97%] purchased from Polycarbon Industries (Devens, MA). Full-coverage OPA SAMs were prepared by spin-coating a 2 mM OPA solution in trichloroethylene (TCE) onto the native oxide surface of a Si wafer and an Al film magnetron-sputtered on a Si wafer, both of which had been cleaned to render the surface hydrophilic by UV/ozone treatment for 1 h. The details for preparing OPA solutions in TCE ready for delivering OPA SAMs on a hydrophilic surface, as well as for characterizations of their coverage, have been documented elsewhere.¹¹

In addition, for comparison with the OPA SAMs on oxidized Si, OPA samples that were not SAMs were also prepared, which we call “free” OPA because the molecules are basically in their native state (of crystalline powder). Such a “free” OPA sample was prepared by putting an excessive amount of OPA powder (e.g., 30 mg) in 5 mL of methanol followed by extending the solution onto a Si wafer. After the solvent evaporated, aggregation of OPA crystalline stacks was seen. Alternatively, the OPA crystalline powder as received could be directly applied to a vacuum-compatible adhesive tap.

A TOF-SIMS IV instrument from ION-TOF GmbH (Münster, Germany) was used to study the differences in the bonding mode of OPA SAMs formed on oxidized Si vs oxidized Al. A 9 keV $^{133}\text{Cs}^+$ primary ion beam produced by surface ionization from a heated cesium pellet source was pulsed with a width of 600 ns and used to bombard the sample to produce secondary ions. These secondary ions, either positive or negative at a time, were extracted by an electric field of 2 kV, and their time-of-flight through a reflectron type of flying tube was measured when they struck, with a postacceleration electric field of 10 kV, on the detector comprised of a scintillator and a photomultiplier tube. After the extraction of the secondary ions was finished, for charge compensation, a low-energy (18 eV) electron beam was flooded on the scanned area until the next pulse of the primary ion beam was shot. All these events were done within

(22) Jespersen, M. L.; Inman, C. E.; Kearns, G. J.; Foster, E. W.; Hutchison, J. E. *J. Am. Chem. Soc.* **2007**, *129*, 2803–2807.

(23) Gadegaard, N.; Chen, X. Y.; Rutten, F. J. M.; Alexander, M. R. *Langmuir* **2008**, *24*, 2057–2063.

(24) Woodward, J. T.; Ulman, A.; Schwartz, D. K. *Langmuir* **1996**, *12*, 3626–3629.

(25) Neves, B. R. A.; Salmon, M. E.; Russell, P. E.; Troughton, E. B., Jr. *Langmuir* **2000**, *16*, 2409–2412.

(26) Schwartz, D. K. *Annu. Rev. Phys. Chem.* **2001**, *52*, 107–137.

(27) Nie, H.-Y.; McIntyre, N. S.; Lau, W. M. *Appl. Phys. Lett.* **2007**, *90*, 203114.

(28) Nie, H.-Y.; McIntyre, N. S.; Lau, W. M.; Feng, J. M. *Thin Solid Films* **2008**, *517*, 814–818.

(29) Hanson, E. L.; Schwartz, J.; Nickel, B.; Koch, N.; Danisman, M. F. *J. Am. Chem. Soc.* **2003**, *125*, 16074–16080.

(30) Nie, H.-Y.; Walzak, M. J.; McIntyre, N. S. *Langmuir* **2002**, *18*, 2955–2958.

(31) Ito, Y.; Virkar, A. A.; Mannsfeld, S.; Joon, H. O.; Toney, M.; Locklin, J.; Bao, Z. *J. Am. Chem. Soc.* **2009**, *131*, 9396–9404.

(32) Hector, L. G., Jr.; Opalka, S. M.; Nitowski, G. A.; Wieserman, L.; Siegel, D. J.; Yu, H.; Adams, J. B. *Surf. Sci.* **2001**, *494*, 1–20.

(33) Pellerite, M. J.; Dunbar, T. D.; Boardman, L. D.; Wood, E. J. *J. Phys. Chem. B* **2003**, *107*, 11726–11736.

(34) Benninghoven, A. *Angew. Chem., Int. Ed.* **1994**, *33*, 1023–1043.

(35) Wandass, J. H.; Gardella, J. A. *J. Am. Chem. Soc.* **1985**, *107*, 6192–6195.

(36) Hagenhoff, B.; Benninghoven, A.; Spinke, J.; Liley, M.; Knoll, W. *Langmuir* **1993**, *9*, 1622–1624.

(37) Wolf, K. V.; Cole, D. A.; Bernasek, S. L. *Anal. Chem.* **2002**, *74*, 5009–5016.

(38) Graham, D. J.; Ratner, B. D. *Langmuir* **2002**, *18*, 5861–5868.

(39) Sohn, S.; Schroder, M.; Lipinsky, D.; Arlinghaus, H. F. *Surf. Interface Anal.* **2004**, *36*, 1222–1226.

(40) Wong, S. C. C.; Lockyer, N. P.; Vickerman, J. C. *Surf. Interface Anal.* **2005**, *37*, 721–730.

(41) Abel, M. L.; Digby, R. P.; Fletcher, I. W.; Watts, J. F. *Surf. Interface Anal.* **2000**, *29*, 115–125.

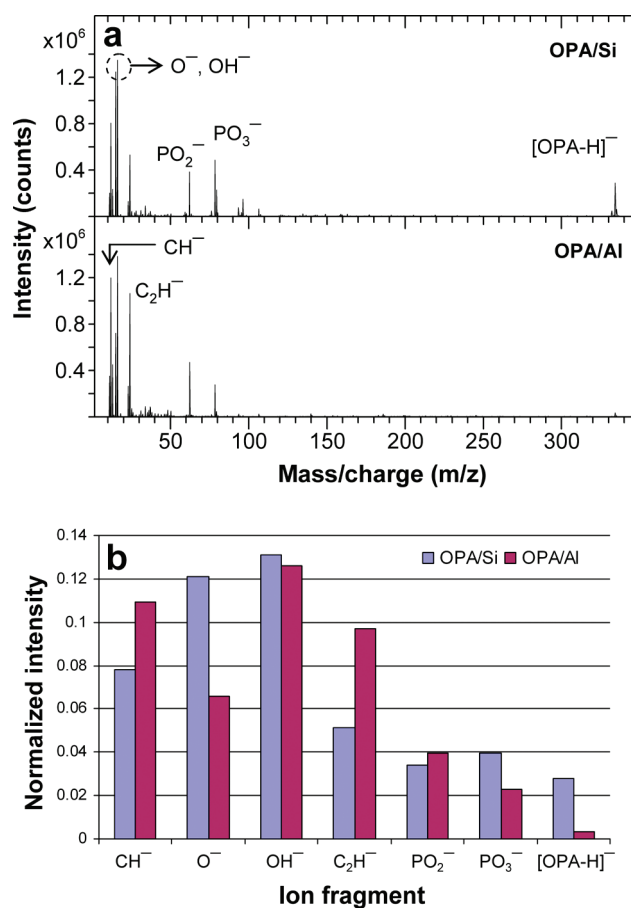


Figure 1. (a) Negative secondary ion mass spectra for OPA/Si (upper panel) and OPA/Al (lower panel), respectively. (b) Normalized ion intensity (to the total ion intensity) for the major ion fragments.

a cycle of 100 μ s (or a repetition rate of 10 kHz), which completes one shot of the primary beam. Many shots could be repeated in order to increase the intensity of the secondary ion fragments. The measured time events of the ion fragments striking the detector were converted to a mass/charge (m/z) ratio via calibration of known species such as hydrogen, carbon, and hydrocarbons. The mass resolution (i.e., the ratio of a mass peak center to the peak width) for the negative and positive OPA molecular ion fragments was $\sim 10\,000$. The base pressure of the analysis chamber of the TOF-SIMS instrument was maintained at $\sim 5 \times 10^{-9}$ mbar.

The target current from the pulsed primary ion beam measured by a Faraday cup was ~ 2 pA, which results in ~ 1200 ions per shot. The primary beam bombarded 128×128 pixels with one shot on each pixel over an area of $500 \mu\text{m} \times 500 \mu\text{m}$ for 112 times. Under these conditions, the primary ion dosage was $\sim 9 \times 10^{11}$ cm^{-2} , which is within the conventional static limit⁴² (because the OPA SAM density is $\sim 4 \times 10^{14}$ cm^{-2}).

RESULTS AND DISCUSSION

Shown in Figure 1a are negative secondary ion mass spectra for OPA SAMs prepared on the native oxide layer of a Si wafer and on an oxidized Al film; for simplicity, these two samples of OPA SAMs are denoted hereafter as OPA/Si and OPA/Al,

respectively. The most abundant ion fragments for both OPA/Si and OPA/Al are CH^- (the measured $m/z = 13.008$), O^- (15.995), OH^- (17.002), C_2H^- (25.007), PO_2^- (62.963), and PO_3^- (78.958). For OPA/Si, the molecular ion fragment $[\text{OPA} - \text{H}]^-$ (333.253) has a comparable intensity to that of PO_2^- and PO_3^- . For OPA/Al, in contrast, $[\text{OPA} - \text{H}]^-$ displays a significantly weaker intensity than that of PO_2^- and PO_3^- . Shown in Figure 1b are the major ion fragments normalized to the total ion intensity, from which their abundance can be compared.

A glance of the results shown in Figure 1 reveals that $[\text{OPA} - \text{H}]^-$ from OPA/Si is much more abundant than that from OPA/Al, though other major fragments are as abundant for both SAMs. Because full-coverage OPA SAMs on both substrates were used for the TOF-SIMS experiment, the lack of abundance of $[\text{OPA} - \text{H}]^-$ from OPA/Al suggests that it is much more difficult for the primary ion beam to generate an OPA molecular ion fragment on OPA/Al than on OPA/Si. For OPA/Al, even though the molecular ion fragment is not abundant, the OPA headgroup ion fragments PO_2^- and PO_3^- are as abundant as their counterparts for OPA/Si. We notice that species fragmented from hydrocarbon chains, such as CH^- and C_2H^- for OPA/Al, are more abundant than those for OPA/Si. These hydrocarbon ion fragments are characteristic species for the alkyl chain of the OPA molecules. It is clear that upon ion bombardment, the OPA molecules in OPA/Al are rather to be decomposed than to be removed, while in OPA/Si, they are removed readily as molecular ion fragments.

The above characteristics in ion fragmentation were also observed in the positive secondary ion mass spectra for both OPA/Si and OPA/Al, as shown in Figure 2a. The ion intensity of the major fragments normalized to the total ion intensity is displayed in Figure 2b. The most abundant ion fragments from the OPA molecules in both samples are CH_3^+ (15.024), C_3H_5^+ (41.042), C_3H_7^+ (43.058), C_4H_7^+ (55.058), and C_4H_9^+ (57.074). In Figure 2b, one sees clearly that the hydrocarbon chain fragments have higher relative intensity for OPA/Al than for OPA/Si. The intensity of $[\text{OPA} + \text{H}]^+$ (335.271) for OPA/Al is much weaker than that for OPA/Si.

Abel et al. reported their TOF-SIMS investigation on organosilane SAMs on an oxidized Al film: the detection of SiOAl^+ reveals chemical bonding between the molecule and the substrate through Si–O–Al linkages.⁴¹ As shown in the lower panel of Figure 2a, we detected POAl^+ (73.953) and POAlH^+ (74.961) on OPA/Al. This is a reflection of the P–O–Al linkage resulting from the condensation reaction between hydroxyl groups both from the OPA headgroup and from oxidized Al.^{16,32,33} However, there is no such counterpart seen on the OPA/Si sample: the dotted line in the upper panel of Figure 2a indicates the m/z (74.945) for fragment POSi^+ , where there is no signal detected.

Shown in Figure 3 is the ion intensity normalized to that of $[\text{OPA} - \text{H}]^-$ for the major negative ion fragments. One can see that for the primary ion bombardment to produce a detected $[\text{OPA} - \text{H}]^-$ for OPA/Al, it generates 7 PO_3^- and 13 PO_2^- . Roughly speaking, among these three negative ions generated from the OPA/Al by the primary ion beam bombardment, less than 5% comes out as $[\text{OPA} - \text{H}]^-$ (when other OPA-related negative ion fragments were included, this number would be even smaller). Therefore, the vast majority of the

(42) Fletcher, J. S.; Lockyer, N. P.; Vaidyanathan, S.; Vickerman, J. C. *Anal. Chem.* **2007**, *79*, 2199–2206.

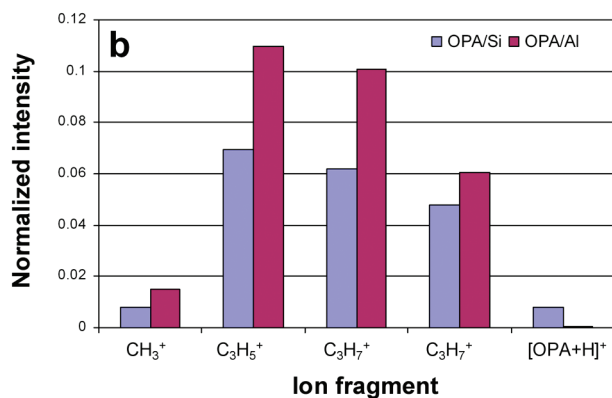
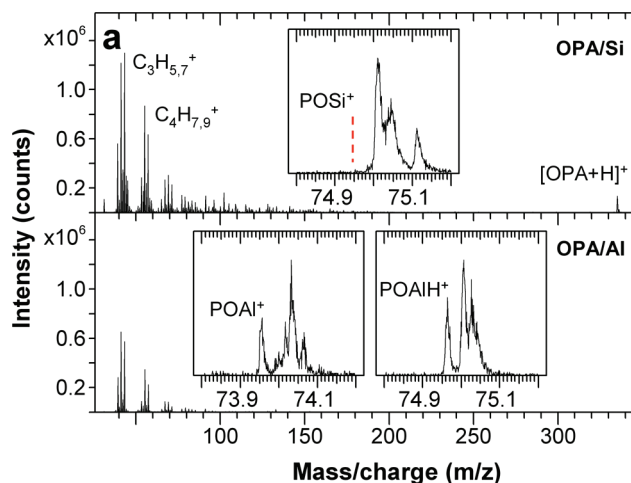


Figure 2. (a) Positive secondary ion mass spectra for OPA/Si (upper panel) and OPA/Al (lower panel). The insert in the upper panels of part a shows the lack of POSi⁺ fragment, which should be at the *m/z* indicated by the dotted line. The insert in the lower panels of part a shows the detection of POAl⁺ and POAlH⁺ fragments. (b) Normalized ion intensity (to the total ion intensity) for the major peaks.

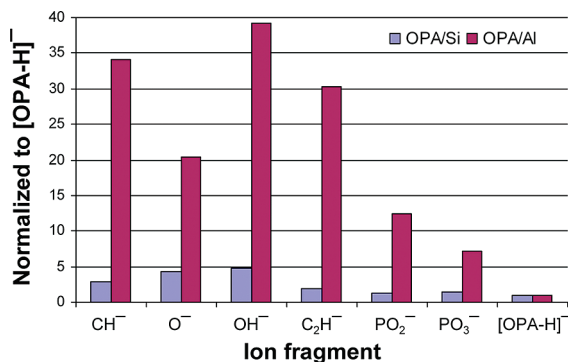


Figure 3. Negative secondary ion mass intensity normalized to that of [OPA - H]⁻ for the major peaks seen on both OPA/Si and OPA/Al.

molecules in OPA/Al are decomposed by the primary ion beam bombardment. In contrast, for OPA/Si, a detected [OPA - H]⁻ accompanies only 1.7 PO₂⁻ and 1.3 PO₃⁻, suggesting that roughly 25% of the OPA molecules in OPA/Si (that are generated as negative ions) are removed as [OPA - H]⁻. The other hydrocarbon fragments and oxygen-containing species are 20–40 times more than [OPA - H]⁻ for OPA/Al but only 2–5 times more than [OPA - H]⁻ for OPA/Si.

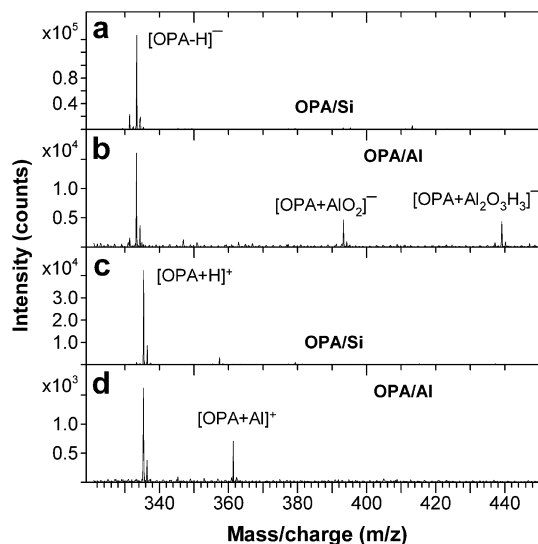


Figure 4. Negative (a, b) and positive (c, d) secondary ion mass spectra for OPA/Si (a, c) and OPA/Al (b, d) in the mass range corresponding to the molecular ion fragment and its association with the substrate constituent element.

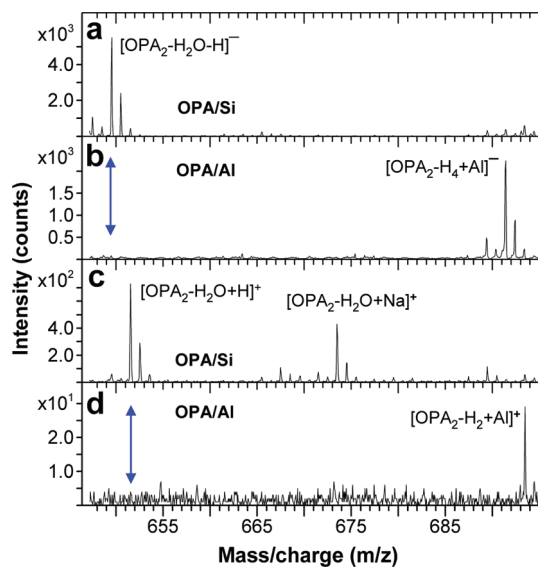


Figure 5. Negative (a, b) and positive (c, d) secondary ion mass spectra for OPA/Si (a, c) and OPA/Al (b, d). The arrows in parts b and d indicate the lack of the condensed dimer from OPA/Al.

Shown in Figure 4 are both negative and positive secondary ion mass spectra for both OPA/Si and OPA/Al in the *m/z* range for the molecular ion fragments and their association with Al (in positive) and its oxide (in negative). For OPA/Si, as shown in parts a and c of Figure 4, the OPA molecular ion fragment dominates. In contrast, for OPA/Al, Figure 4b shows that the two OPA molecular ion fragments associated Al oxides, [OPA + AlO₂]⁻ (393.211) and [OPA + Al₂O₃H₃]⁻ (439.169), are relatively strong in comparison with [OPA + H]⁻. As shown in Figure 4d, the OPA molecular ion associated with Al, [OPA + Al]⁺ (361.243), is roughly half of the intensity of [OPA + H]⁺.

The observations on ion fragmentation of OPA SAMs presented so far in this article suggest that the bonding mode of OPA molecules in OPA/Si is different from that in OPA/Al. However, the defining evidence for revealing the bonding mode for OPA/

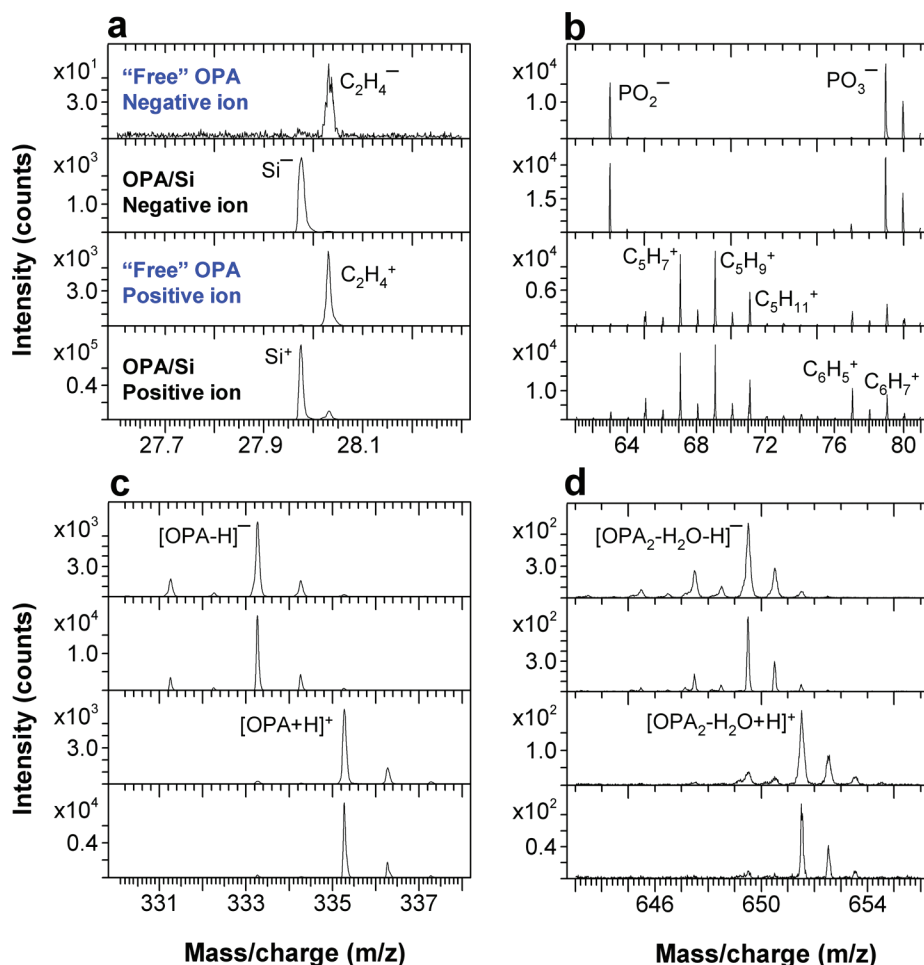


Figure 6. Negative and positive secondary ion mass spectra for “free” OPA and OPA/Si. The first and second panels in parts a–d are the negative ion spectra for “free” OPA and OPA/Si, respectively. The third and fourth panels in parts a–d are the positive ion spectra for “free” OPA and OPA/Si, respectively. The denotations for the “free” OPA and OPA/Si samples in part a are true for parts b–d.

Si is the detection of OPA condensed dimer, which is the product of condensation of two OPA molecules with the loss of a water molecule and is observed as both negative (Figure 5a) $[\text{OPA}_2 - \text{H}_2\text{O} - \text{H}]^-$ (649.499) and positive (Figure 5b) $[\text{OPA}_2 - \text{H}_2\text{O} + \text{H}]^+$ (651.530) ion fragment. This condensed OPA dimer is absent on OPA/Al (parts b and d of Figure 5b). Therefore, the detection of the condensed dimer ion fragments serves to identify the presence of OPA molecules that are not covalently bonded to the substrate.

On OPA/Al, as shown, respectively, in parts b and d of Figure 5, there is a characteristic OPA dimer associated with Al, detected as negative $[\text{OPA}_2 - \text{H}_4 + \text{Al}]^-$ (691.416) and positive $[\text{OPA}_2 - \text{H}_2 + \text{Al}]^+$ (693.480) ion fragments. This observation indicates that an Al atom is attached to three oxygen atoms of the three hydroxyl groups of two OPA molecules, replacing the three hydrogen atoms. This characteristic ion fragment is even seen for OPA SAMs formed on freshly cleaved Muscovite mica, where Al is a constituent beneath the cleaved mica surface.⁴³ Interestingly, as shown in Figure 5c, on OPA/Si, one sees $[\text{OPA}_2 - \text{H}_2\text{O} + \text{Na}]^+$ (673.511), which is a reflection of contamination of the rather mobile sodium ion. The contamination is believed to be caused by the weakly bonded nature of the OPA SAMs

on the oxidized Si, which is wettable as verified by water contact angle measurements.¹¹ In contrast, this species is virtually unseen on OPA/Al, which is nonwetable. Therefore, the sodium contamination observed by TOF-SIMS on OPA/Si provides a unique insight to relating the bonding mode of the molecules to the substrate with the chemical stability of their SAMs.

We now try to understand the significance of the condensed OPA dimer and its implication on TOF-SIMS being an analytical technique to reveal the bonding mode of OPA SAMs on an oxide. On the basis of the experimental results shown in Figure 5, we propose that one can use the detection of or the lack of the condensed OPA dimer as a criterion to judge whether the OPA molecules in their SAMs are bonded to the substrate by H-bonding or by a covalent bond. In order to make sense of this reasoning, we carried out TOF-SIMS experiments on OPA molecules in their native state (i.e., in the form of crystalline powder), where there is perhaps H-bonding, but no strong chemical bonding, between the OPA headgroups since the OPA powder dissolves easily in alcohols and melts at 100 °C. We refer to OPA molecules in their native form of powder as “free” OPA, in the sense that the molecules are not covalently bonded to each other or to anything else. Indeed, as shown in Figure 6 for both the negative and positive secondary ion mass spectra obtained on the “free” OPA

(43) Francis, J. T.; Nie, H.-Y.; McIntyre, N. S.; Briggs, D. *Langmuir* 2006, 22, 9244–9250.

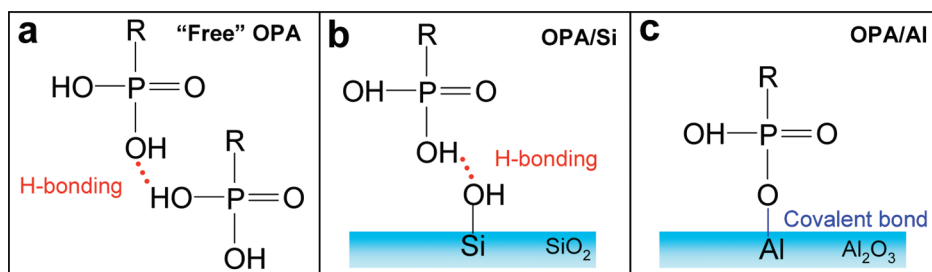


Figure 7. Schematic illustration of OPA molecules in (a) “free” OPA, (b) OPA/Si, and (c) OPA/Al. R represents OPA’s alkyl chain of $\text{CH}_3(\text{CH}_2)_{17}$. There is no difference between parts a and b in terms of bonding of an OPA molecule to a hydroxyl group (H-bonding). In contrast, an OPA molecule in OPA/Al is covalently bonded through the P–O–Al linkage.

sample and the OPA/Si sample, we have confirmed that the OPA-related ion fragmentation from the “free” OPA sample resembles that seen on the OPA/Si sample.

As shown in Figure 6a, the “free” OPA sample was thick enough so that there is no Si^- (the first panel) and Si^+ (the third panel) ions detected on the OPA molecules aggregated over a Si substrate. In comparison, as shown, respectively, in the second panel for negative and the forth panel for positive ion mass spectra, these two ions are detected on the OPA/Si sample with decent intensity, because the OPA monolayer is only ~ 2 nm in thickness, while the penetrating depth of the primary ion beam is on the order of 10 nm. Therefore, by checking the (lack of) Si signals coming from the Si substrate, we verified that the “free” OPA sample represent the bulky OPA powder, which is an aggregate of OPA molecules bonded by van der Waals forces between the alkyl chains and H-bonding between the headgroups of the molecules.

Figure 6b–d shows that the characteristic OPA ion fragmentation from the “free” OPA sample is identical to that from OPA/Si, i.e., the weakly bonded OPA SAMs on oxidized Si. Especially, as shown in Figure 6d, we have proven that the detection of condensed OPA dimer $[\text{OPA}_2 - \text{H}_2\text{O} - \text{H}]^-$ and $[\text{OPA}_2 - \text{H}_2\text{O} + \text{H}]^+$ provides an analytical criterion for TOF-SIMS to reveal a bonding mode where OPA molecules lack strong chemical bonds to each other in their aggregates (the “free” OPA sample) or to the substrate in their SAMs (the OPA/Si sample). These experimental results elucidate that the OPA molecules in OPA/Si are attached to the surface with strength similar to that between OPA molecules in their aggregates, which is probably H-bonding in nature between the OPA molecular headgroups. This TOF-SIMS analysis on OPA/Si and “free” OPA verifies the observations that the OPA SAMs are easily attacked by water and alcohols and are not strongly bonded to the oxidized surface of a Si wafer.^{11,16,29}

As for the origin of the condensed OPA dimer, it is unlikely that condensation reaction between the OPA molecules (homocondensation) occurs in air at room temperature; the OPA molecules may do so at elevated temperatures.¹⁶ The vacuum and/or the ion bombardment must have promoted homocondensation of OPA molecules, under the condition that the OPA molecules be in a bonding mode lacking strong chemical bonding.

On the basis of analyses on our TOF-SIMS results, the bonding modes of OPA molecules in “free” OPA, OPA/Si, and OPA/Al can be depicted in Figure 7. As shown in parts a and b of Figure 7, the bonding modes for OPA molecules with each other in “free” OPA (powder) and with the substrate in OPA/Si are the same, i.e., H-bonding. This bonding mode is manifested by the detection of the condensed OPA dimer in TOF-SIMS.

On the other hand, as shown in Figure 7c, OPA molecules in OPA/Al possess a totally different bonding mode, where they are covalently bonded to the substrate via the P–O–Al linkage, resulting from condensation reaction between the hydroxyl group of the OPA headgroup and the hydroxyl group on oxidized Al.^{16,32,33} In this case, there are no “free” OPA molecules available for the generation of condensed OPA dimers in TOF-SIMS.

CONCLUSIONS

We have elucidated that OPA molecules in OPA SAMs on oxidized Si are as “free” (i.e., no strong chemical bonding involved) as they are in OPA crystalline powder (the native state of the chemical), which serves as evidence that the OPA molecules in their SAMs are weakly bonded to oxidized silicon, likely via H-bonding. The TOF-SIMS signature for such “free” OPA molecules is detection of condensed OPA dimer, i.e., two OPA molecules combined with the loss of a water molecule. In contrast, for covalently bonded OPA SAMs on oxidized Al, the condensed OPA dimer is absent. Therefore, our TOF-SIMS results have revealed a phenomenon: the generation of condensed OPA dimer by the primary ion bombardment requires the presence of “free” OPA molecules. This finding provides TOF-SIMS an analytical criterion for revealing the bonding mode of organophosphorus acid molecules in their SAMs on oxides.

ACKNOWLEDGMENT

The author is indebted to Drs. Stewart McIntyre and Leo Lau of Surface Science Western for their support to this research and insightful discussion on surface chemistry and to Dr. James Francis for technical discussion.

Received for review March 15, 2010. Accepted March 18, 2010.

AC100671Q